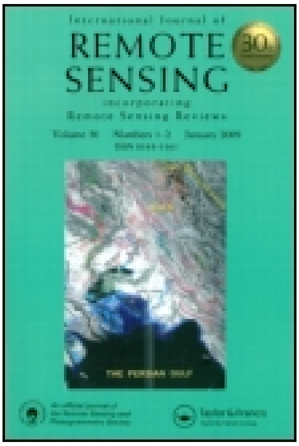

International Journal of Remote Sensing
Publication details, including instructions for authors and subscription information:
http://www.tandfonline.com/loi/tres20

Super-resolution mapping of the waterline from remotely sensed data

Giles M. Foody [a] , Aidy M. Muslim [a] & Peter M. Atkinson [a]
[a] School of Geography, University of Southampton, Highfield, Southampton, SO17 1BJ, UK
Published online: 22 Feb 2007.

International Journal of Remote Sensing
Vol. 26, No. 24, 20 December 2005, 5381–5392

Super-resolution mapping of the waterline from remotely sensed data

GILES M. FOODY*, AIDY M. MUSLIM and PETER M. ATKINSON
School of Geography, University of Southampton, Highfield, Southampton, SO17 1BJ, UK

(*Received 12 August 2003; in final form 16 June 2005*)

Methods for mapping the waterline at a subpixel scale from a soft image classification of remotely sensed data are evaluated. Unlike approaches based on hard classification, these methods allow the waterline to run through rather than between image pixels and so have the potential to derive accurate and realistic representations of the waterline from imagery with relatively large pixels. The most accurate predictions of waterline location were made from a geostatistical approach applied to the output of a soft classification (RMSE=2.25 m) which satisfied the standards for mapping at 1 : 5000 scale from imagery with a 20 m spatial resolution.

1. Introduction

As the boundary between land and water surfaces, the waterline is one of the most basic and common features represented on maps. It can, however, be difficult to map accurately, particularly if the water body is dynamic. Remote sensing has been used widely to map the waterline. A variety of data sets and methods have been used, but typically the waterline is mapped through image classification procedures, including density slice analysis (Ryan *et al*. 1991, Gorman *et al*. 1998, Moore 2000, Frazier and Page 2000, Pajak and Leatherman 2002, Stockdon *et al*. 2002, Horritt *et al*. 2003). Although land and water generally appear to be spectrally separable in many of the wavebands used widely in remote sensing, the accuracy of waterline prediction is sometimes low. In particular, spectral confusion, arising notably from effects such as those due to variable depth and turbidity, together with the spatial resolution of the imagery, which influences the clarity of boundaries and proportion of mixed pixels, limits the accuracy of waterline mapping (Barrette *et al*. 2000, Frazier and Page 2000, Ryu *et al*. 2002, Malthus and Mumby 2003, Thomson *et al*. 2003).

Mapping from remotely sensed imagery is commonly achieved through the application of a conventional hard image classification analysis. With hard classification, each pixel in the image is allocated to the class with which it has the greatest similarity spectrally. The effect of this allocation process is to constrain the prediction of inter-class boundaries to lie between pixels. Since the size and location of pixels in an image are independent of the ground cover mosaic, it is unlikely that the pixels are arranged in such a manner that their edges correspond sufficiently to inter-class boundaries on the ground for hard classification to be an appropriate basis for mapping from many image data sets. In reality,

*Corresponding author. Email: g.m.foody@soton.ac.uk

International Journal of Remote Sensing
ISSN 0143-1161 print/ISSN 1366-5901 online © 2005 Taylor & Francis
http://www.tandf.co.uk/journals
DOI: 10.1080/01431160500213292

the boundary between classes will generally run through the area represented by a pixel, with the pixel having a mixed class composition. Since hard classification can allocate a pixel to only one class its application will have the effect of mislocating boundaries, such as the waterline, with an error that is generally positively related to the pixel size.

Commonly, relatively fine-to-moderate spatial resolution imagery (e.g. 20 m SPOT HRV, 30 m Landsat TM/ETM+) that provides an inexpensive means of mapping a large area in a regularly updatable manner has been used in waterline mapping (Frazier and Page 2000). The spatial resolution of these systems, however, limits the ability to map and monitor small (subpixel scale) changes in waterline position. While the new generation of very fine spatial resolution sensors (e.g. IKONOS) offers increased spatial resolution, the imagery from such systems is often inappropriate for many users, particularly if a large area is to be mapped (Mumby and Edwards 2002). Thus, if constrained to use fine-to-moderate spatial resolution (>10 m) imagery, there is a desire to map the waterline at a subpixel scale. In such situations the aim is, therefore, to derive a map that depicts the feature of interest at a scale finer than the data set from which it was derived, which may be achieved through a super-resolution analysis (Tatem *et al.* 2001, Verhoeye and De Wulf 2002).

Here, preliminary results of an investigation to derive super-resolution maps of the waterline are presented. The approach is based on the outputs of a soft rather than conventional hard classification. Soft classification is used since it allows a pixel to have multiple and partial class memberships and so can accommodate the effects of mixed pixels. The conventional output of a soft classification is a set of fraction images which indicate the relative coverage of the classes in the area represented by the pixel. If these predicted class covers could be located geographically within the area represented by the pixel, it would allow the boundary between classes to be plotted at a subpixel scale. The main aim of this paper is to investigate approaches for fitting the waterline to a soft classification derived from remotely sensed imagery.

2. Data

A 500 m long stretch of coast in Kampng Seberang Takir, Terengganu, Malaysia, was used (figure 1). The coast at this site had an approximately linear shape, orientated at about 45° to the pixel grid of the imagery used to ensure that the waterline ran through pixels. Since the aim was to investigate the accuracy of subpixel scale mapping of the waterline, the study used a very fine spatial resolution IKONOS image to locate the actual position of the boundary with the super-resolution analyses undertaken on a spatially degraded version of this image. Although imperfect, this approach removes problems of misregistration between the image to be classified and the reference data on waterline position. The approach also ensures the spectral correspondence of the data used at each spatial resolution.

The IKONOS image of the test site was acquired in July 2000 with a spatial resolution of approxiniately 1 m (figure 1(*a*)). From this image, the position of the

Figure 1. Test site. (*a*) Black and white representation of the IKONOS image with a 1 m spatial resolution and (*b*) simulated image with a 20 m spatial resolution. The same scale and orientation are used in these and later illustrations and the grid coordinates are given in terms of the Malaysian RSO projection.

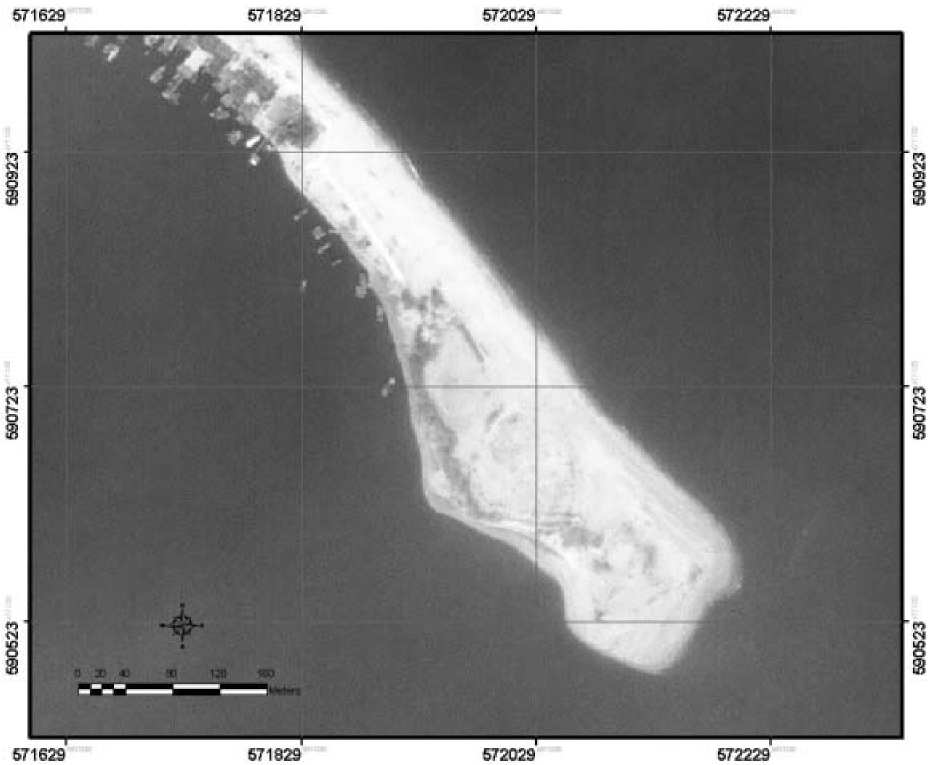
571629
571829
572029
572229
590923
590723
590523
0 20 40 80 120 160
Meters

(*a*)

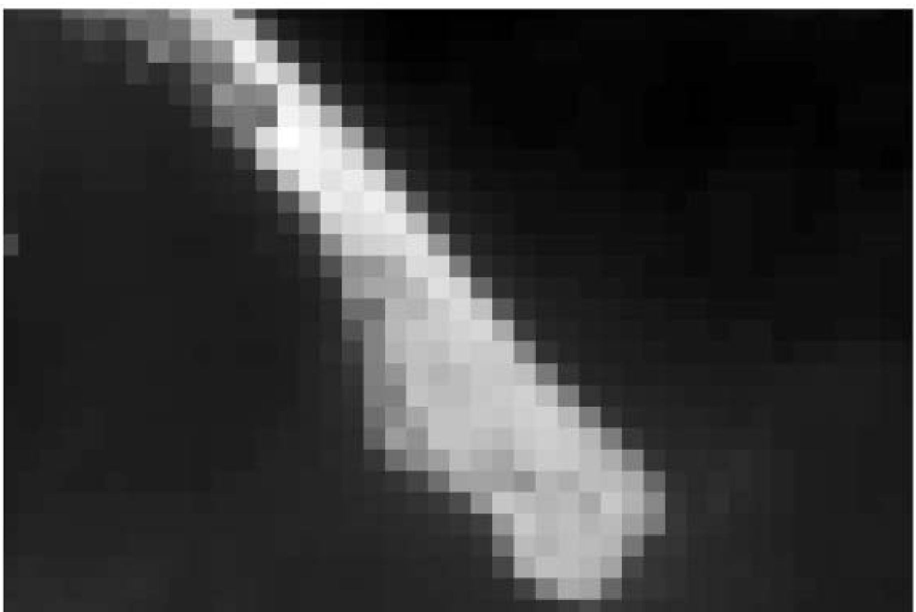

(*b*)

waterline was mapped using a conventional maximum likelihood classification trained on data drawn from a set of large homogeneous blocks of land and water cover located either side of the coastline studied. This classifier was selected as a standard and widely available technique for hard image classification. While this classification forced the waterline to lie between pixels the small size of the pixels in relation to the spatial frequency of variation in waterline position ensured that this was not a source of major error.

The IKONOS image was degraded spatially by aggregating pixels to yield a simulated image with a spatial resolution of 20 m (figure 1(*b*)), comparable to that of commonly used satellite remote sensor data (e.g. SPOT HRV). Since the simulated image was to be used to predict waterline location using classification analyses which may be evaluated against that derived from the original image, the effect of noise reduction in the spatial degradation was countered by adding noise to ensure that the signal-to-noise ratio of the simulated image was similar to that of the original image. The signal-to-noise ratio was estimated using a geostatistical method based on the variogram (Smith and Curran 1999). Predictions of the waterline location were derived from the simulated image with a spatial resolution of 20 m using three methods.

3. Waterline mapping

The waterline was mapped from the simulated imagery with a series of classification-based methods. The same training sites were used in all the classifications.

As a benchmark, a conventional hard classification was used to predict the waterline from the simulated image. The waterline was fitted to the derived output of this classification by threading it between pixels allocated to the different classes.

The alternative approaches to mapping the waterline were all based on soft classification. Here, a soft classification depicting the two classes, land and water, was derived using a sigmoidal class membership function. For this, pure land and water responses were derived from the training data and applied to the end points of the class membership function (figure 2). The function was then used to derive a soft classification in which the output comprised the strength of predicted membership of each pixel to the land class. For each pixel, this fuzzy membership value derived indicated its relative degree of membership to the two classes. For a pixel with a large degree of mixing, the fuzzy membership value derived was treated as representing the proportion of the pixel's area that was covered with land, while the remainder was ascribed to the water class.

The output of the soft classification for each pixel was an indication of the relative membership to the two classes and, in the area where membership was greatly mixed, this was taken as an estimate of the proportional cover of the component classes (figure 3). This output does not indicate the location of the subpixel component covers within the area represented by the pixels, information that is required to fit a class boundary at a subpixel scale. Since there was a simple geometrical arrangement of the two classes, the possibility of representing the waterline by fitting a class membership contour through the soft classification was evaluated (Foody 2002, Foody *et al.* 2003). Specifically, the waterline was represented by fitting to the output of the soft classification a contour of 0.50 membership to the land class, representing the 50% membership to land and 50%

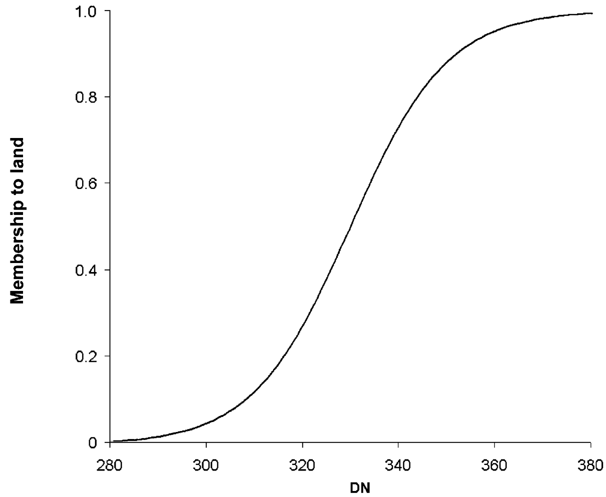

Figure 2. The fuzzy membership function used to derive the soft classification.

membership to water scenario. This approach has been used previously to locate coastal features at a subpixel scale (Foody 2002).

Although the contour fitted to the soft classification output may locate the boundary more accurately than conventional methods and convey additional information on boundary properties such as its sharpness (Foody *et al.* 2003), a significant disadvantage of the contour-based approach to waterline mapping is that

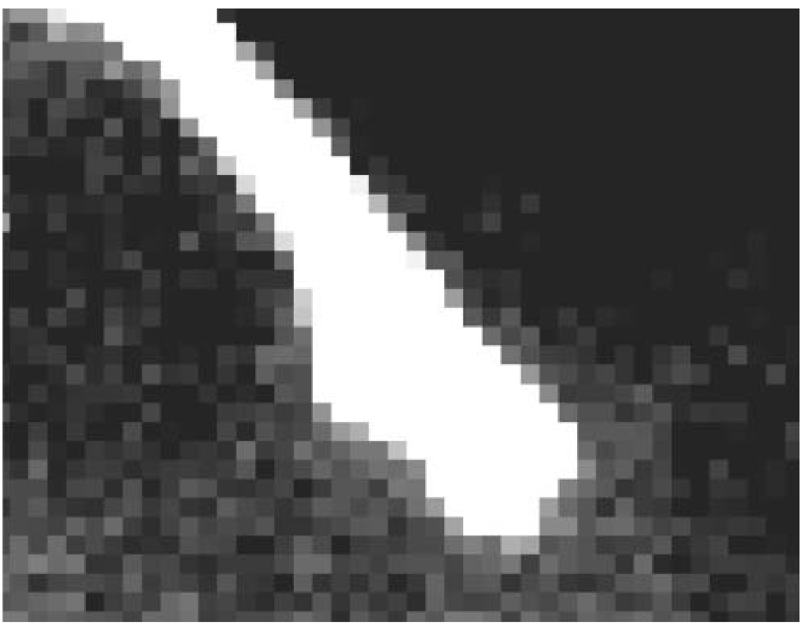

Figure 3. Soft classification derived with the application of the function shown in figure 2 from the simulated image shown in Figure 1(*b*). The grey scale indicates the degree of membership to the land class that was treated as an estimate of the proportional coverage of land (white=complete land cover, black=complete water cover).

the class compositional information provided by the soft classification is not maintained in fitting the contour. That is, the contour fitted to the soft classification is guided by the class proportional information conveyed by the soft classification but the proportions either side of the fitted boundary may not match those depicted in the soft classification as a result of the generalization process involved in fitting the contour. A refinement, therefore, is to use the derived contour to direct an approach in which the class proportional information contained in the soft classification is maintained. This was achieved here by applying a geostatistical pixel swapping algorithm (Atkinson 2004) inspired by simulated annealing to the soft classification, guided by the contour fitted to it, to predict the location of the waterline. This approach used a spatial optimization algorithm based on the two-point histogram or grey-level co-occurrence matrix (Deutsch and Wen 1998). For a random variable z that can take one of k=1,…,K outcomes (i.e. classes), the two-point histogram for a particular lag (distance and direction of separation) **h** is the set of all bivariate transition probabilities

$$p_{k,k'(h)} = \Pr\left\{ \begin{array}{l} z(\mathrm{u}) \in k, \\ z(\mathrm{u}+\mathrm{h}) \in k' \end{array} \right\}$$

Independent of location **u**, for all k, k'=1,…K. The objective function corresponding to the two-point histogram control statistic is

$$O = \sum_{\mathrm{h}} \left(\sum_{k=1}^{K} \sum_{k'=1}^{K} \left[p_{k,k'}^{training}(\mathrm{h}) - p_{k,k'}^{realization}(\mathrm{h}) \right]^2 \right)$$

where $p_{k,k'}^{training}(\mathrm{h})$ are the target transition probabilities calculated from a training image and $p_{k,\,k'}^{realization}(\mathrm{h})$ are the corresponding transition probabilities of the realization image. Here, the training image is the representation derived from the contour fitted to the soft classification. The realization image is the representation derived from an iteration of the algorithm. Together with an algorithm to swap subpixel values within the area represented by a pixel in the 20 m spatial resolution image, the two-point histogram may be used to increase the spatial resolution of the data. This method ensured that the proportions of land and water predicted by the soft classification were maintained while geographically locating subpixel-sized regions of the classes in the area represented by a pixel (Atkinson 2004). Here, the analysis was undertaken using subpixels with a spatial resolution of 2.5 m. In essence, therefore, the geostatistical approach was used to adjust iteratively the location of the subpixel class composition estimates in the soft classification output to provide a super-resolution representation of the waterline.

The waterlines predicted from each of the three methods applied to the simulated image were compared with that derived from the classification of the original, 1 m spatial resolution, image. To provide an estimate of the accuracy of waterline mapping, the distance between the predicted and actual location of the waterline was calculated at each metre point along the coast. As our aim was to evaluate super-resolution mapping approaches for locating a boundary at a subpixel scale and not to define a particular boundary, the focus throughout this study was on mapping the instantaneous waterline (that apparent at the time of image acquisition) and not, for example, the land–sea boundary that exists at a specific tidal state, which is often the boundary represented on maps. By timing image acquisition in relation to tidal conditions or using a model of the terrain surface it

Table 1. Closeness of predicted waterline to actual indicated by RMSE, percentage of predictions within 2 m (10% of pixel dimension) of the actual waterline and the distance from the actual waterline containing 90% of predictions.

Mapping method	RMSE (m)	Within 2m (%)	90% within (m)
Hard classification	6.48	25.8	10.0
Contouring soft classification	3.20	35.4	5.0
Geostatistical approach	2.32	68.4	3.6

may be possible to adjust the instantaneous waterline to represent an alternative boundary if desired, but this is beyond the scope of the current article.

4. Results and discussion

The waterline was mapped from the outputs of both the hard and soft classifications applied to the simulated image. The accuracy of the shoreline predictions was assessed relative to the shoreline predicted from the classification of the original, 1 m spatial resolution, image.

The hard classification of the simulated image provided the least accurate representation of the waterline (table 1, figure 4). The waterline produced by the hard classification had a jagged shape, as it was constrained to lie between pixels, and provided an inadequate visual representation of the waterline. Moreover, only

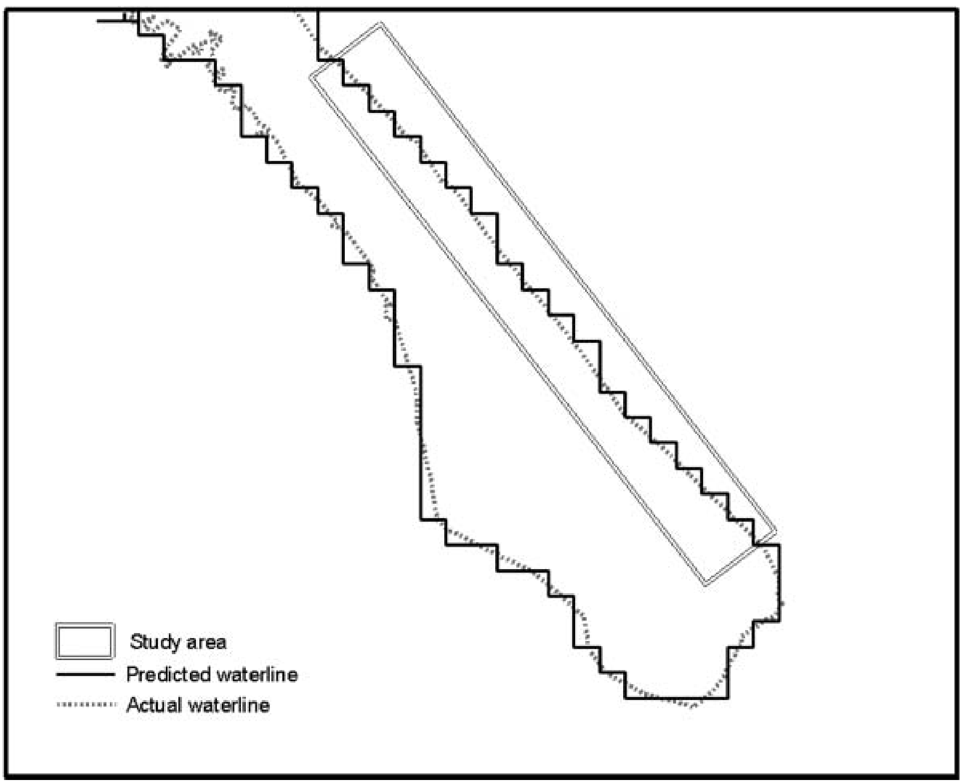

Figure 4. Waterline predicted from the hard classification applied to the simulated image.

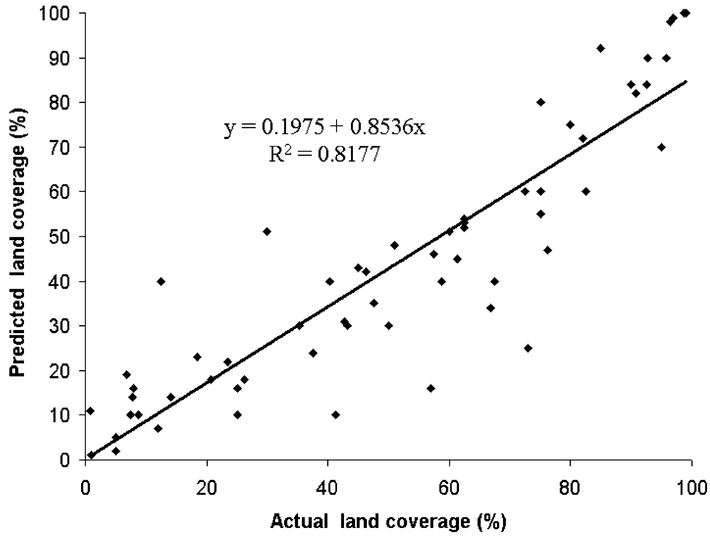

Figure 5. Relationship between the proportional cover of land (expressed as a percentage) predicted from the soft classification and that derived from the reference data.

25.8% of the waterline predicted was within 2 m of the actual waterline and the RMSE calculated along the 500 m test site was 6.48 m.

The soft classification (figure 3) provided an alternative representation for the waterline mapping. Since this soft classification was the basis of all the super-resolution analyses, its accuracy was evaluated by comparing the predicted coverage of a class with that derived from the reference data, the classified 1 m spatial resolution image. The correlation between the actual and predicted coverage was $r=0.904$ (figure 5), and hence the soft classification was taken to be an appropriate base for the super-resolution analyses. The waterline predictions derived from the two approaches applied to the output of the soft classification provided more realistic and accurate representations than the hard classification. Figure 6 indicates the relative accuracy of the approaches for the test site.

The waterline predicted from the contour fitted to the soft classification provided, visually and quantitatively, a more realistic representation than that derived from the hard classification (figure 7, table 1). For example, 35.4% of sites lay within 2 m

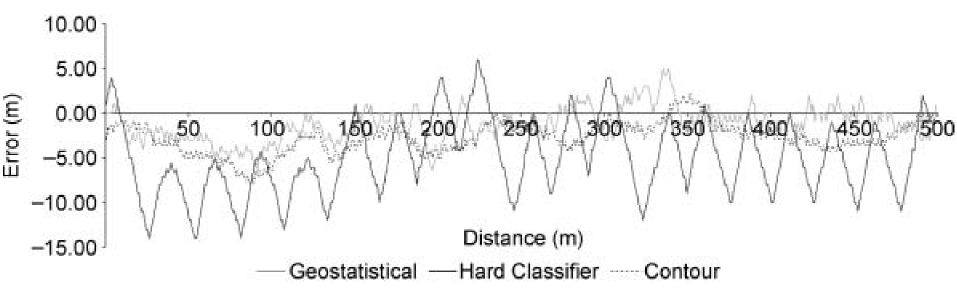

Figure 6. Error in waterline prediction from the three methods applied to the simulated image along the 500 m stretch of coast studied. Positive errors indicate the waterline was plotted in water while negative errors indicate it was plotted inland.

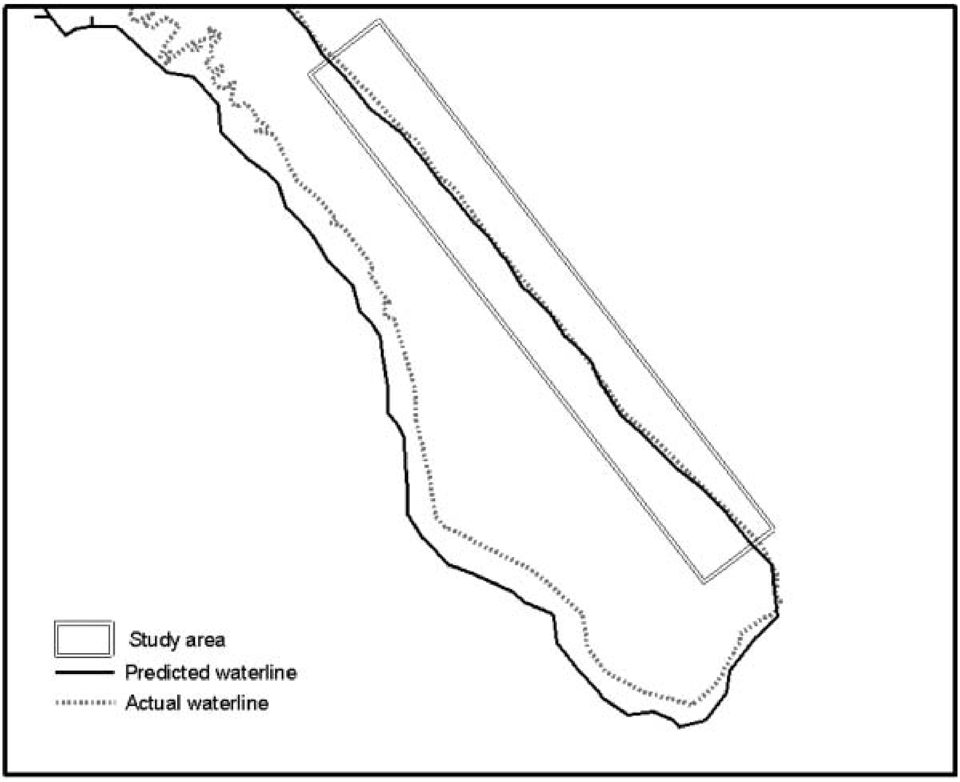

Figure 7. Waterline predicted by the contour fitted to the soft classification of the simulated image. Note that the fit is inaccurate outside of the study area, sites distant from the location of the training sites, indicating the impact of local variations in variables such as water depth and turbidity on the mapping.

of the prediction derived from the original image. Note, however, that predictions outside the study area were relatively inaccurate. It is likely that the training statistics used, especially for the water class, were less representive of the class than in the study area and this is an issue to be addressed in future research.

The waterline predicted from the geostatistical approach provided the most accurate and visually realistic representation (table 1, figure 8). The RMSE derived from this analysis was 2.25 m and 68.4% of the predicted waterline lay within 2 m of the actual waterline.

The accuracy of the waterline predictions may also be evaluated from the perspective of traditional mapping standards. The US National Map Accuracy Standard for maps with a cartographic scale of 1 : 20 000 or larger demands that at least 90% of a sample of well-defined points plotted lie within 1/30 th inch of the correct position when plotted on the map. Taking the sites along the waterline as forming such a sample for illustrative purposes, all the waterline predictions derived, including that from the hard classification, appear to satisfy this requirement for mapping at a scale of 1 : 20 000 (table 1). However, the predictions from the geostatistical approach satisfied the standards at map scales larger than 1 : 20 000. For example, 90% of the waterline predicted using the geostatistical approach was within 3.6 m of the actual waterline position, satisfying the map accuracy standard for 1 : 5000 scale maps. The results indicate the

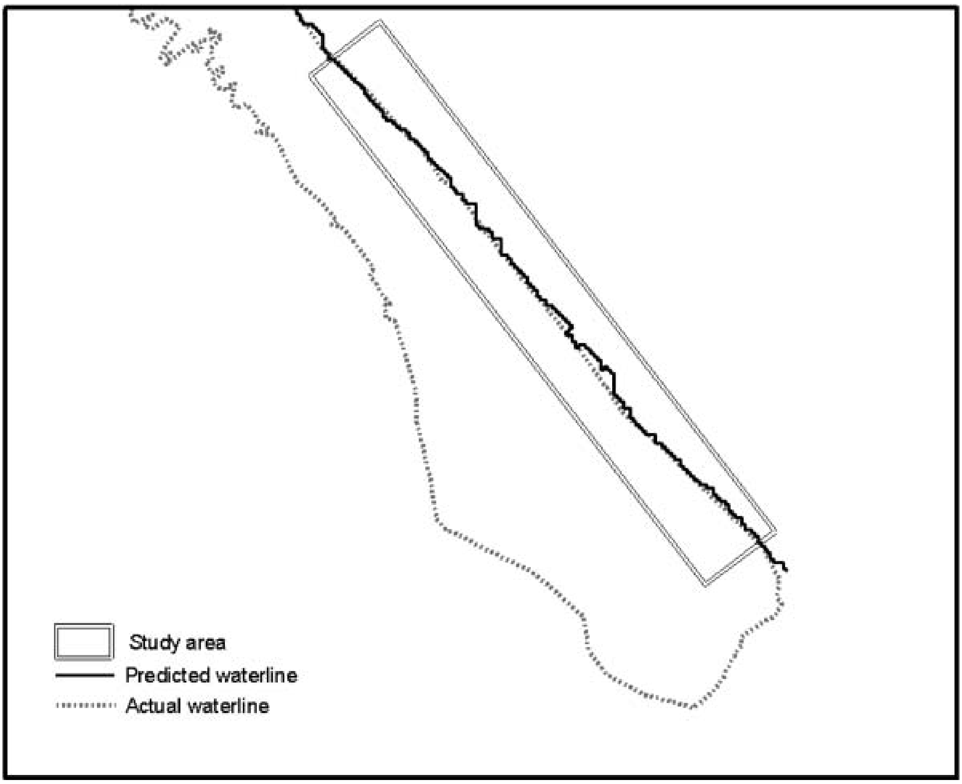

Figure 8. Waterline predicted from the geostatistical approach applied to the soft classification of the simulated image.

considerable potential of super-resolution mapping techniques for locating boundaries such as the waterline from remotely sensed data. More rigorous evaluation, preferably with field-surveyed ground data on boundary location is, however, required. Further research is also required to determine the broader applicability of super-resolution mapping techniques to data from different sensors and to different boundary types as well as to accommodate effects such as geographical variation in class response and the representativeness of training statistics.

5. Summary and conclusions

Boundaries such as the waterline cannot be represented appropriately in a conventional approach to thematic mapping from remotely sensed data based on hard classification, as their location is constrained by the data's pixel grid. Predictions of the thematic composition of a pixel derived from a soft classification may, however, be located geographically and used to fit the boundary at a subpixel scale. This allows super-resolution mapping, mapping at a scale finer than the spatial resolution of the data used, which can provide more accurate and realistic thematic representations. This was illustrated with the mapping of the waterline from simulated data with a 20 m spatial resolution.

The conventional hard classification provided a visually inadequate and quantitatively inaccurate representation of the waterline. A superior representation, in terms of visual appearance and RMSE, was derived from each of the super-resolution mapping approaches applied to the soft classification. Thus, the accurate representation of the sub-pixel proportional land cover composition conveyed in the soft classification ($r=0.904$) could be used to direct the fitting of the waterline at a subpixel scale. The simple approach based on fitting a contour to the soft classification yielded a more realistic and accurate representation of the waterline than the hard classification. In fitting the contour, however, the subpixel class compositional information was not maintained. An alternative approach based on simulated annealing and using a geostatistical pixel-swapping algorithm, which maintained the class compositional information and which was initialized with the contour location, provided the most accurate waterline representation. With the geostatistical approach, the predicted waterline position was sufficient to satisfy the US National Mapping standards at a scale of 1 : 5000.

Although these results indicate the considerable potential of super-resolution mapping techniques for waterline mapping, further research is required. Current research is addressing the applicability of the methods to waterlines of more complicated shape and with a wider range of land/sea contrast than investigated here.

Acknowledgements

We are grateful to the Malaysian Government/Malaysian Centre for Remote Sensing for their generous support and provision of a research scholarship to A.M.M. This article is based on a paper presented at IGARSS'03, Toulouse. We are also grateful to the two referees for their constructive comments on the manuscript.

References

Atkinson, P.M., 2004, Super-resolution land cover classification using geostatistical optimization. In *GeoENV IV: Geostatistics for Environmental Applications*, X. Sánchez-Vila, J. Carrera and J. Gomez-Hernandez (Eds), pp. 15–28 (Dordrecht: Kluwer).

Barrette, J., August, P. and Golet, F., 2000, Accuracy assessment of wetland boundary delineation using aerial photography and digital orthophotography. *Photogrammetric Engineering and Remote Sensing*, **66**, pp. 409–416.

Deutsch, C.V. and Wen, X.H., 1998, An improved perturbation mechanism for simulated annealing simulation. *Mathematical Geology*, **30**, pp. 801–816.

Foody, G.M., 2002, The role of soft classification techniques in the refinement of estimates of ground control point location. *Photogrammetric Engineering and Remote Sensing*, **68**, pp. 897–903.

Foody, G.M., Jackson, R.G. and Quine, C.P., 2003, Potential improvements in the characterisation of forest canopy gaps caused by windthrow using fine spatial resolution multispectral data: comparing hard and soft classification techniques. *Forest Science*, **49**, pp. 444 – 454.

Frazier, P.S. and Page, K.J., 2000, Water body detection and delineation with Landsat TM data. *Photogrammetric Engineering and Remote Sensing*, **66**, pp. 1461–1467.

Gorman, L., Morang, A. and Larson, R., 1998, Monitoring the coastal environment. IV. Mapping, shoreline changes, and bathymetric analysis. *Journal of Coastal Research*, **14**, pp. 61–92.

Horritt, M.S., Mason, D.C., Cobby, D.M., Davenport, I.J. and Bates, P.D., 2003, Waterline mapping in flooded vegetation from airborne SAR imagery. *Remote Sensing of Environment*, **85**, pp. 271–281.

Malthus, T.J. and Mumby, P.J., 2003, Remote sensing of the coastal zone: an overview and priorities for future research. *International Journal of Remote Sensing*, **24**, pp. 2805–2815.

Moore, L.J., 2000, Shoreline mapping techniques. *Journal of Coastal Research*, **16**, pp. 11–124.

Mumby, P.J. and Edwards, A.J., 2002, Mapping marine environments with IKONOS imagery: enhanced spatial resolution can deliver greater thematic accuracy. *Remote Sensing of Environment*, **82**, pp. 248–257.

Pajak, M.J. and Leatherman, S., 2002, The high water line as shoreline indicator. *Journal of Coastal Research*, **18**, pp. 329–337.

Ryan, T.W., Sementilli, P.J., Yuen, P. and Hunt, B.R., 1991, Extraction of shoreline features by neural nets and image processing. *Photogrammetric Engineering and Remote Sensing*, **57**, pp. 947–955.

Ryu, J.-H., Won, J.-S. and Min, K.D., 2002, Waterline extraction from Landsat TM data in a tidal flat. A case study in Gomso Bay, Korea. *Remote Sensing of Environment*, **83**, pp. 442–456.

Smith, G.M. and Curran, P.J., 1999, Methods for estimating image signal-to-noise ratio (SNR). In *Advances in Remote Sensing and GIS Analysis*, P.M. Atkinson and N.J. Tate (Eds), pp. 61–74 (Chichester: Wiley).

Stockdon, H.F., Sallenger, A.H., List, J.H. and Holman, R.A., 2002, Estimation of shoreline position and change using airborne topographic lidar data. *Journal of Coastal Research*, **18**, pp. 502–513.

Tatem, A.J., Lewis, H.G., Atkinson, P.M. and Nixon, M.S., 2001, Super-resolution land cover pattern prediction using a Hopfield neural network. *Remote Sensing of Environment*, **79**, pp. 1–14.

Thomson, A.G., Fuller, R.M., Yates, M.G., Brown, S.L., Cox, R. and Wadsworth, R.A., 2003, The use of airborne remote sensing for extensive mapping of intertidal sediments and saltmarhes in eastern England. *International Journal of Remote Sensing*, **24**, pp. 2717–2737.

Verhoeye, J. and De Wulf, R., 2002, Land cover mapping at the sub-pixel scale using linear optimisation techniques. *Remote Sensing of Environment*, **79**, pp. 96–104.